Intrinsic Josephson Effects in $Bi_2Sr_2CaCu_2O_8$ Single Crystals

R. Kleiner, F. Steinmeyer, G. Kunkel, and P. Müller

Walther-Meissner-Institut, Walther-Meissner-Strasse 8, W-8046 Garching, Germany

(Received 21 August 1991; revised manuscript received 11 February 1992)

We have observed Josephson coupling between CuO double layers in $Bi_2Sr_2CaCu_2O_8$ single crystals by direct measurements of ac and dc Josephson effects with current flow along the c axis. The results show that a small $Bi_2Sr_2CaCu_2O_8$ single crystal behaves like a series array of Josephson junctions which can exhibit mutual phase locking.

PACS numbers: 74.50.+r, 74.60.Jg, 74.70.Jm

The theory of layered oxide superconductors focuses on the possible types of coupling within the essential structure elements: the CuO planes. However, independent of the exact nature of the pairing mechanism within the layers, the *interlayer* coupling determines most of the superconducting properties of a real crystal. To date it is not clear how the Cooper pairs move across the interlayer spacing. In $Bi_2Sr_2CaCu_2O_8$ (BSCCO) the upper critical magnetic fields are so large that the standard anisotropic Ginzburg-Landau theory yields c-axis coherence lengths ξ_c of the order of 1 Å [1]. This is much less than the distance of 12 Å between the CuO double layers. Therefore, the Lawrence-Doniach picture would be more appropriate [2], i.e., BSCCO should be described as a set of discrete superconducting layers whose order parameters are coupled by Josephson interaction. Several theories [2,3] and recent experiments concerning the angle dependence of the critical current [4] and the torque [5] support this idea. A convincing proof, however, can only be given by direct measurements of ac and dc Josephson effects [5]. The simplest model of a BSCCO superconductor is a stack of superconducting sheets consisting of the CuO bilayers separated by the BiO and SrO layers acting as weak links or as insulators. Experimentally we therefore have to consider series arrays of proximity [superconductor-normal-metal-superconductor (SNS)] or tunneling [semiconductor-insulator-semiconductor (SIS)] Josephson junctions and pay attention to the following points.

(1) If the c-axis supercurrents are limited by the Josephson effect, the I-V characteristics exhibit a concave curvature in the resistive state. If, on the other hand, the supercurrents are limited by flux flow, this curvature is convex. Therefore the I-V characteristics give first-hand information whether or not the supercurrents are of the Josephson type.

(2) If the (ab)-plane dimensions of the Josephson junctions are larger than the Josephson penetration length λ_j, Josephson vortices can be formed in the barrier. Whereas in standard tunnel junctions λ_j is governed by the magnetic self-fields of the Josephson currents, in BSCCO λ_j is dominated by the kinetic momentum of the current flow along the (ab) axes, because the thickness of the electrodes (i.e., the CuO double layers) is much smaller than the field penetration depth along the c axis ($\lambda_{ab} \approx 3000$ Å) [6]. The Lawrence-Doniach theory yields $\lambda_j = \gamma t$, where t is the interlayer spacing and γ is the penetration depth anisotropy ratio [7]. For BSCCO $\lambda_c \approx 100$ μm [8], which yields $\lambda_j \approx 0.4$ μm.

(3) In standard tunnel junctions with an electrode thickness larger than the magnetic field penetration depth and ab dimensions smaller than λ_j, I_c vs H should follow a Fraunhofer pattern, $I_c(H) = I_c(0)|\sin(x)/x|$, with $x = \pi\mu_0(2\lambda + t)wH/\Phi_0$. w is the junction width perpendicular to $\mathbf{H}$, t is the barrier thickness, and λ is the magnetic penetration depth. In BSCCO the factor $(2\lambda + t)$ has to be replaced by the distance between the midpoints of the electrodes [7,9], approximately 15 Å in BSCCO. Therefore the field scale of the I_c modulations is drastically increased. For $w = 0.5$ μm the first zero of the critical current occurs in a field of 2.7 T. For $w = 30$ μm this value decreases to 0.5 kOe. In this case, however, $I_c(H)$ is influenced by the formation of Josephson vortices. In addition, because of the extreme anisotropy and the large field scale, even a misalignment of 0.1° of the crystals may lead to the formation of Abrikosov vortices [5] within the CuO double layers, which will also influence the I_c vs H pattern.

(4) Josephson coupling can be established via tunneling (SIS) or proximity effects (SNS). The two types of junctions have different dependences of the critical current I_c on temperature. Therefore I_c vs T measurements can determine whether the junctions are of SIS or SNS type.

(5) Whereas the dc measurements determine the properties of single junctions, interactions between different junctions can be studied through ac measurements. These interactions may be due to electromagnetic or quasiparticle coupling in the resistive state. They can lead to mutual phase locking, if the spread in the junction parameters is small enough [10,11]. In that case, in external microwave fields of frequency f current steps of integer order n occur at voltages $V_n = Nnhf/2e$, with N the number of phase-locked junctions [12]. Phase locking of as many junctions as possible separates intrinsic Josephson effects from spurious ones arising from, for instance, cracks in the crystal, since it is unlikely that different random junctions can have almost identical properties.

(6) Self-synchronization in microwave emission experiments also supports the existence of intrinsic junctions. Phase-locked junctions will radiate with bandwidths N times smaller than single Josephson junctions [10].

In order to test these ideas we have performed the above measurements on BSCCO single crystals of typi-

 © 1992 The American Physical Society

cally 30×30 μm^2 in the a-b direction and 3 μm in the c direction corresponding to a stack of approximately 2000 Josephson junctions. The crystals were grown from a stoichiometric mixture of the oxides, heated up to 980 °C and then cooled down to 800 °C at a rate of 1 °C/h. Gold contacts were evaporated on both sides of the crystals; this was followed by an anneal in Ar (12 h at 600 °C) or O_2 (36 h at 400 °C). The contact resistivities were typically 10^{-4} Ωcm^2 permitting a two-terminal measuring technique. The in-plane resistivities ρ_{ab} of our samples ranged between 150 and 250 $\mu\Omega$ cm at room temperature with a positive temperature coefficient down to T_c. The c-axis resistivities ρ_c of our samples strongly depend on the annealing conditions. The Ar annealed samples (*Fa*,*Id*,*C*,*F*,*M*, and *E*) had $\rho_c(T_c)$ of 10–20 Ω cm with a quasi-semiconducting-dependence on temperature. The critical current densities j_c(4.2 K) varied between 100 and 200 A/cm^2 and T_c between 85 and 87 K. The transition widths ΔT_c ranged between 2 and 4 K. Sample *J*, annealed in O_2, had $\rho_c(T_c)=5$ Ω cm with a positive temperature coefficient above 150 K and a negative temperature coefficient at lower temperatures. j_c(4.2 K) was approximately 300 A/cm^2, T_c was 83 K, and $\Delta T_c \approx 3$ K. The most significant difference between the Ar and O_2 annealed samples is the anisotropy factor γ [5,6], as determined by angular resolved torque measurements [13]. It varied from 50 for O_2 annealed samples up to 280 for Ar anneal.

For the magnetic field measurements the crystals were oriented by a two-axis goniometer. The microwave absorption experiments (2–18 GHz) were performed in Cu cavities. For the emission experiments the crystals were mounted inside a horn at the end of an *X*-band waveguide. The signal was preamplified and mixed down with a local oscillator at 10 GHz. Then the signal was either monitored by a tuned uhf receiver at a fixed frequency or the spectral distribution was analyzed. The basic sensitivity of the spectrum analyzer was -130 dBm at a bandwidth of 1 MHz.

A typical I-V characteristic at $T=4.2$ K is shown in Fig. 1. Increasing the bias current beyond I_c leads to several finite voltage jumps. If the current is then decreased, the voltage first changes continuously until it jumps back to a lower value, and can be increased continuously again. Ramping the current up and down repeatedly yields many discrete branches of the I-V characteristics. We have discerned more than a hundred different branches at successively higher voltages, the limit given by Ohmic heating of the crystal. At higher temperatures the hystereses decrease and disappear above $T=70$ K.

The shapes of the resistive branches are similar to the I-V characteristics of small underdamped Josephson junctions [14] rather than to the zero-field steps observed in large junctions [15]. In the latter case at increasing bias currents the branches should rapidly tend to current steps which are due to the resonant motion of vortex-antivortex pairs. In contrast to that we always observe a finite resistance increasing with the branch number at fixed bias current. The curvature of the branches can well be explained by the V-shaped quasiparticle conductance observed in c-axis tunneling experiments [16]. Therefore we conclude that the different branches are due to an increasing number of junctions in the resistive state, with every single junction having a hysteretic I-V characteristic.

We note that in Fig. 1 most of the branches are almost equally spaced, except for a few cases, where one branch lies close to another. In our opinion the neighboring equally spaced branches differ by one junction in the resistive state. Physically different groups, each having the same number of junctions, result in branches lying close together. From this assumption we derive an average characteristic voltage $V_c=I_cR_n$ of 13 mV for the sample under discussion (R_n: resistance of the junction in the normal state). For SIS tunnel junctions, $V_c=\pi/2\Delta$. A gap value Δ of 12 meV [17] yields $V_c=19$ meV which is not too far from our measured value. The Ar annealed samples had V_c's between 5 and 15 mV, whereas the V_c's for O_2 annealed samples ranged between 0.5 and 1 mV. Some of our samples exhibited I-V characteristics with much less pronounced hystereses and characteristic voltages in the μV regime, possibly due to parasitic shunt resistances (cf. Fig. 4).

In the following we will discuss the temperature and field dependences of the critical currents. In order to

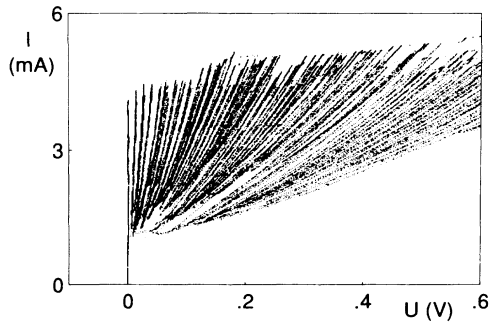

FIG. 1. I-V characteristic of sample *Fa* at $T=4.2$ K. The contact resistance of 18 Ω is subtracted.

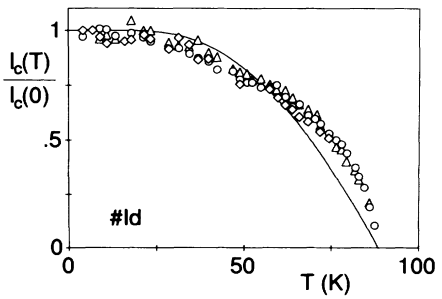

FIG. 2. I_c vs T of sample *Id*, taken from the first three branches of the I-V characteristic. Solid line: BCS theory (see text).

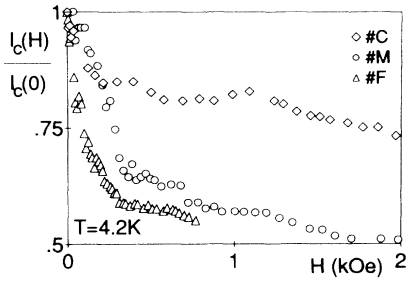

FIG. 3. I_c vs H for three different samples at 4.2 K. The data were taken from the first branch of the I-V characteristic.

avoid interactions between the junctions we examined only the first few branches of the I-V characteristics. Figure 2 shows I_c vs T of sample Id. Near T_c the data are above the values for SIS tunnel junctions given by the Ambegaokar-Baratoff relation, $I_cR_n = \pi/2\Delta(T) \times \tanh[\Delta(T)/2k_BT]$, with $\Delta(T)$ from the BCS theory (solid line in Fig. 2). At low temperatures they intersect the SIS curve. We have calculated $\Delta(T)$ from our data by inverting the Ambegaokar-Baratoff relation. The obtained $\Delta(T)$ stays constant almost up to T_c and is in excellent agreement with the energy gap obtained from Raman data [17,18].

Figure 3 shows I_c vs H of three different samples. The data exhibit modulations on a 0.5-kOe field scale with shallow minima in I_c. Assuming that the first steep I_c decrease is determined by the geometric scale of the junction, we can derive junction widths w from our data, which conform with the crystal dimensions measured by a scanning electron microscope. Therefore we conclude that the Josephson junctions are indeed formed by two adjacent CuO double layers.

We have seen Shapiro steps only in the I-V characteristics of those samples having small hystereses and characteristic voltages of the less than 100 μV (corresponding to characteristic frequencies $f = V_c/\Phi_0$ of less than 50 GHz). The voltage spacings of the steps indicate that groups of several tens of junctions are phase locked.

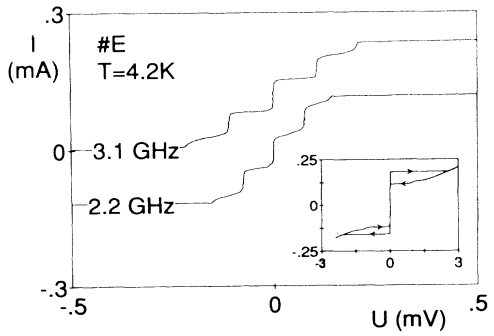

FIG. 4. I-V characteristics of sample E at two different microwave frequencies. The 3.1-GHz curve is vertically offset. Inset: The I-V characteristic at zero power using the same units. The contact resistance of 2.4 Ω is subtracted.

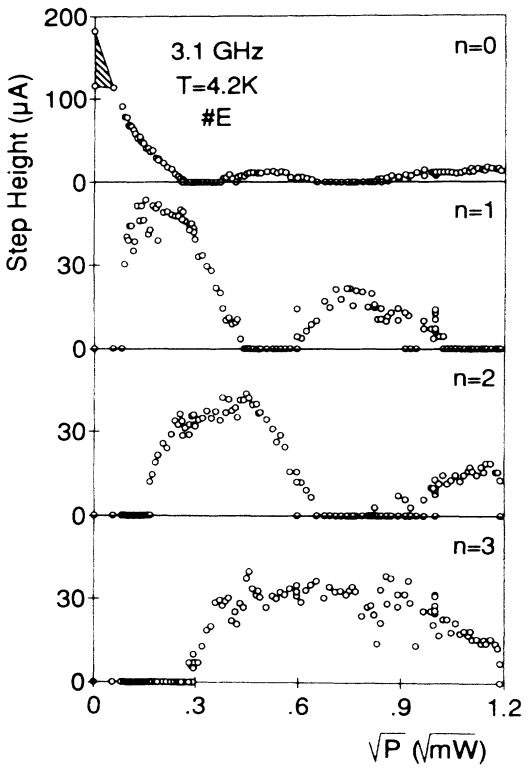

FIG. 5. Height of the Shapiro steps $n=0$ to $n=3$ of sample E vs $P^{1/2}$. The shaded area denotes the hysteretic region.

Figures 4 and 5 show an example for $N=17$. With increasing microwave power P the hysteresis vanishes and Shapiro steps appear. The steps shift directly proportional to the frequency in accordance with the Josephson voltage-frequency relation (Fig. 4) and remain phase locked over a wide power range. The step heights are symmetric with respect to positive and negative bias currents. As a function of microwave power they are modulated similar to the behavior of a single junction (Fig. 5). The gaps between the step maxima are typical for hysteretic junctions.

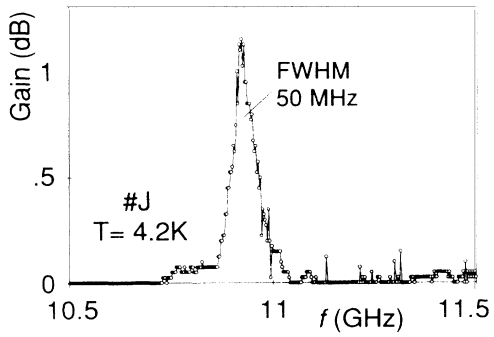

FIG. 6. Power spectrum of the microwave emission at a voltage where coherent emission occurs. Unity gain is set at −123.8 dBm. The measured points are connected by lines to guide the eye.

To date we have observed Shapiro steps resulting from up to 200 junctions in series. However, in most cases they appear only in small frequency and power ranges interrupted by unstable and chaotic regimes. Such chaotic behavior is also well known from underdamped Josephson junctions [19].

The above results are further confirmed by our microwave emission experiments. Clearly, X-band emission can only be observed from crystals with low V_c and small hysteresis, i.e., from O_2 annealed samples. Monitoring the emitted power at fixed frequency as a function of the voltage across the crystal we find several sharp peaks and a broad background. The spectral linewidth (FWHM) of the broad part at a fixed voltage is approximately 300 MHz, however, only 50 MHz at the peaks (Fig. 6). A linewidth of 300 MHz is typical for a single Josephson junction [10]. As mentioned above this linewidth decreases as $1/N$ for N phase-locked junctions. We therefore argue that the broad emission comes from unlocked Josephson junctions whereas at the peaks several junctions radiate coherently. Because of the unknown number of junctions radiating incoherently we cannot directly deduce the number of phase-locked junctions from the voltage-frequency relation. However, from the ratio of the linewidths of the coherent and the incoherent part, in most of our experiments we estimate a number of phase-locked junctions of the order of 10.

To conclude, our results give strong evidence for Josephson coupling between the CuO double layers in BSCCO. The observation of groups of several tens of phase-locked junctions as well as the observation of several hundred equidistant branches in the I-V characteristics rule out spurious effects. The anisotropy as well as the junction parameters can be controlled by the oxygen stoichiometry. Although our results are strongly influenced by crystal imperfections they show the possibility of using small BSCCO single crystals as naturally grown series arrays of Josephson junctions.

We wish to thank Dr. W. Wersing, Siemens AG, München, and H. Hagn, Physik Department E17, TU München, for technological support.

[1] M. J. Naughton, R. C. Yu, P. K. Davies, J. E. Fischer, R. V. Chamberlin, Z. Z. Wang, T. W. Jing, N. P. Ong, and P. M. Chaikin, Phys. Rev. B **38**, 9280 (1988).
[2] J. Appel and D. Fay, Phys. Rev. B **41**, 873 (1990).
[3] M. Tachiki, S. Takahashi, F. Steglich, and H. Adrian, Z. Phys. B **80**, 161 (1990).
[4] P. Schmitt, P. Kummeth, L. Schultz, and G. Saemann-Ischenko, Phys. Rev. Lett. **67**, 267 (1991).
[5] F. Steinmeyer, R. Kleiner, and P. Müller, Physica (Amsterdam) **185-189C**, 2381 (1991); R. Kleiner, F. Steinmeyer, G. Kunkel, and P. Müller, *ibid.* **185-189C**, 2617 (1991).
[6] A. Schilling, F. Hulliger, and H. R. Ott, Z. Phys. B **82**, 9 (1991).
[7] L. N. Bulaevskii, J. R. Clem, and L. I. Glazman, Phys. Rev. B (to be published).
[8] J. R. Cooper, L. Forro, and B. Keszei, Nature (London) **343**, 444 (1990).
[9] M. Weihnacht, Phys. Status Solidi **32**, K169 (1969).
[10] A. K. Jain, K. K. Likharev, J. E. Lukens, and J. E. Sauvageau, Phys. Rep. **109**, 309 (1984).
[11] P. Hadley, M. R. Beasley, and K. Wiesenfeld, Phys. Rev. B **38**, 8712 (1988).
[12] D. W. Palmer and J. E. Mercereau, Appl. Phys. Lett. **25**, 467 (1974).
[13] F. Steinmeyer, R. Kleiner, and P. Müller (to be published).
[14] D. E. McCumber, J. Appl. Phys. **39**, 3113 (1968).
[15] T. A. Fulton and R. C. Dynes, Solid State Commun. **12**, 57 (1973).
[16] D. Mandrus, L. Forro, D. Koller, and L. Mihaly, Nature (London) **351**, 460 (1991).
[17] M. Boekholt, M. Hoffmann, and G. Güntherodt, Physica (Amsterdam) **175C**, 127 (1991).
[18] T. Staufer, R. Nemetschek, R. Hackl, P. Müller, and H. Veith, Phys. Rev. Lett. **68**, 1069 (1992); R. Hackl, R. Kleiner, and P. Müller (to be published).
[19] R. L. Kautz and R. Monaco, J. Appl. Phys. **57**, 875 (1985).